Investigation of Friction Stir Processing for defect free microstructural refinement of Magnesium alloy

Gaurav Kumar Sharma[1], Kamal Kumar[2], Navneet Thakur[3]

{gkvats5@gmail.com[1], kamaljangra@pec.edu.in[2], navneetthakur71@gmail.com}

Department of Mechanical Engineering
Punjab Engineering College (Deemed to be University)[1,2,& 3]

Abstract. A solid-state material processing method called friction stir processing (FSP) is primarily utilized to enhance mechanical characteristics, eliminate casting defects, and refine grains. In present study FSP parameters namely tool rotational speeds (560, 710, and 900 rpm) and tool tilt angles (0° and 1.5°) have been investigated for microstructural refinement of Mg-2Zn Mg-alloy. The traverse speed kept constant at 25 mm-min^{-1}. The results showed that the FSP performed at low tool rotational speed of 560 and 710 rpm in combination 0° tilt angle yielded structural defects, whereas rotation speed of 900 rpm and tilt angle 1.5° resulted into defect free microstructure and significant grain refinement from 63.86 µm to 27.38 µm, and microhardness improvement from 47 HV to 58 HV. The electrochemical corrosion resistance of FSP processed Mg-2Zn Mg-alloy was deteriorated as compared with the as-rolled Mg-2Zn Mg-alloy after 24 hrs.

Keywords: FSP, Mg-2Zn Mg-alloy, microstructure, corrosion rate, grain refinement.

1 Introduction

Recent years have observed a lot of interest in magnesium (Mg) alloys owing to their exceptional biocompatibility, low density, and high specific strength. [1]–[3]. However, magnesium alloys suffer with poor corrosion resistance, which limits their applications in certain environments[4]. This problem is mainly due to the higher electronegativity of Mg^{+} and microstructural defects developed during the casting process [5], [6]. Friction stir processing (FSP), as illustrated in Fig. 1(a), is an environmental-friendly and solid-state process that has been extensively utilized to improve mechanical characteristics and microstructural refinement of Mg-alloys [7]–[9]. FSP can also be useful to enhance the corrosion resistance of Mg-alloys by suitable powder reinforcements [10]–[12]. During FSP, a rotating tool inserted into a workpiece and moves along the workpiece to create a solid-state deformation zone. The deformation zone leads to grain refinement and texture alteration, which can remarkably enhance the mechanical properties of the alloy [13], [14].

Recent study on FSP of AZ61 Mg alloy revealed the improvement in microhardness (54 HV to 73 HV), grain size refinement and enhanced yield strength (YS) (57 MPa to 80 MPa), ultimate tensile strength (UTS) (159 to 302 MPa) along with greater elongation (12.2 to 26.4%) [15]. Yijie Hu et al [16] observed the tunnel defect during FSP of ZK60 Mg alloy with tool rotational speed of 500 rpm and traverse speed of 100 mm/min, while defect free and

ICAMDMS 2024, February 23-24, Coimbatore, India

DOI 10.4108/eai.23-2-2024.2347028

refined microstructure was obtained with rotational speed of 800 rpm to 1400 rpm and traverse speed of 50 to 100 mm/min. Dialami N. et. al [17] performed FSP simulation and obtained the defect free processed zone with tool tilt angle of 2.5°. Most of the studies considered the effective range of tool tilt angle from 1° to 3°. Tool tilt angle plays crucial part to generate the optimized heat generation, improved stirring action and proper material flow to generate a defect free and refined microstructure. Tool tilt angle above 3° produces negative impact and generate FSP defects like tunnelling, lack of surface filling, worm hole and flash etc.

In a recent research Mehrian S. et. al [18] evaluated corrosion behaviour of FSP treated Al-Mg alloy under different cooling mediums and found that FSP had a positive impact on corrosion rate. Patel et. al [19] carried out a preliminary electrochemical potentiodynamic study on FSP treated AZ31B Mg alloy and untreated material. It was reported that corrosion potential for untreated or base material (BM) and FSPed alloy remained nearly similar (0.546 V), whereas the corrosion current density was lower for FSP treated alloy (2.032×10^{-3} A/cm^2) compared to BM (9.815×10^{-3} A/cm^2). The available studies on the influence of FSP on corrosion resistance are inconsistent and the detailed study on corrosion behavior of Mg alloys after FSP treatment is not well understood.

Mg-2Zn Mg-alloy is biocompatible material highly suitable for biodegradable implant applications. But research work on FSP treatment of Mg-2Zn Mg-alloy is currently missing. Therefore, in this study, FSP treatment has been performed on Mg-2Zn alloy to explore the effect of tool rotational speeds and tool tilt angles to get defect-free and refined microstructures.

2 Experimental procedures

As-cast Mg-2Zn Mg alloy plates of thickness 4.5 mm were used in current study. The plates were sectioned in the size of 30 mm x 210 mm, for FSP treatment. The FSP tool was made of H13 tool steel. Tool's shoulder diameter and pin diameter were 18 mm and 6 mm respectively, whereas length of the pin was 3 mm. Table 1 and table 2 represent the chemical composition of as-cast Mg-2Zn and FSP parameters that were employed in this investigation, respectively.

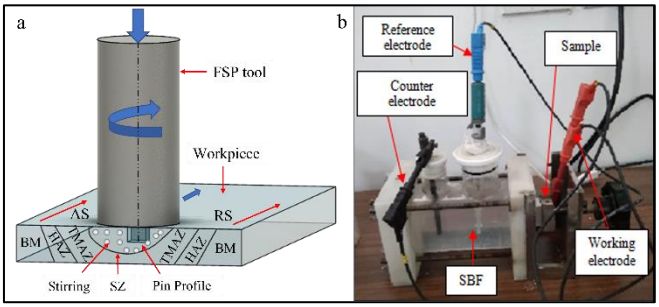

Fig 1 (a) Schematic diagram of FSP (b) Electrochemical corrosion measurement cell

Following the FSP process on the Mg-2Zn alloy, SiC paper was used to polish the samples, and ethanol was used for cleaning. The surface and structural defects were analyzed using the

stereo-zoom microscope (Stemi 508, make: Germany) and the microstructures were taken using optical microscope. For microstructure evaluation, polished and cleaned samples were etched using picral etchant (70 ml ethanol ,10 ml acetic acid, 10 ml demineralized H_2O and 4 g picric acid). The microhardness was carried out at micro-Vickers hardness tester for 10 seconds and 100g load. Corrosion rate (CR) of FSP treated and untreated samples were measured using electrochemical polarization techniques.

Table 1. Mg-2Zn alloy's composition.

Element	Ca	K	Zn	Mg
%	0.063	0.070	1.572	Balance

Table 2. Process parameters employed in current study

Parameter	**Symbol**	**Value**
Tool rotation speed (rpm)	TRS	560, 710, 900
Transverse speed (mm/min)	TTS	25
Tool tilt angle	TA	0°, 1.5°

Electrochemical workstation (shown in Fig. 1(b), make: Autolab) was used for corrosion measurements. The measurements were executed in the simulated body fluid (SBF) solution at room temperature.

3 Results and discussion

FSP executed on Mg-2Zn Mg-alloy using tool tilt angle (TA) of 0° in combination with TRS of 560 and 710 rpm has generated defects like; surface lack of fill and tunnelling defects. However, FSP at TRS; 900 rpm, and TTS of 25 mm-min^{-1} with TA; 1.5° has produced a defect free processed zone in Mg-alloy. The defect free processed zone was further examined for grain refinement, microhardness and CR.

3.1 Defects Analysis

As shown in Fig. 2, surface lack of fill defect generated during FSP at TA; 0° and TRS of 560 rpm, and 710 rpm which was attributed to the low heat-generation and less material stirring. According to the equation (1) [16], heat generation is highly dependent on rotational speed (ω) of FSP tool.

$$\boldsymbol{T = K\left(\frac{\omega^2}{\upsilon * 10^4}\right)^{\alpha} * T_m} \qquad \textbf{(1)}$$

Where; T- deformation temperature, ω – TRS, υ- TTS, T_m – melting point of alloy, K and α are the constants having values 0.8052 and 0.8052 respectively.

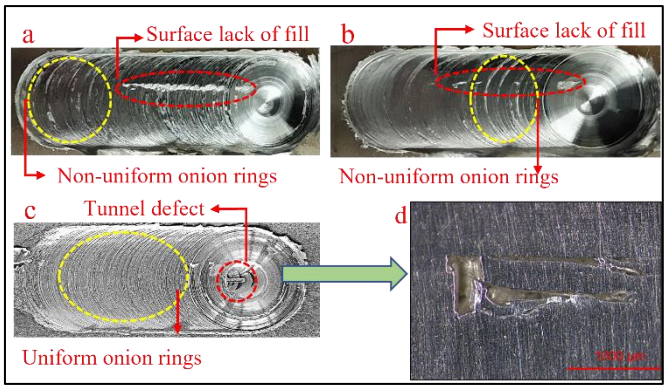

Fig 2 Various defects occurred during FSP of Mg-2Zn Mg-alloy (a) surface lack of fill at 560 rpm, 0° and 25 mm/min, and (b) at 710 rpm, 0° and 25 mm/min, (c) tunnel defect at 900 rpm, 0° and 25 mm/min (d) stereo zoom image of the tunnel defect

Fig 3 Defect free FSP processed sample at 900 rpm, 1.5° and 25 mm/min

Apart from low TRS, TA; 0° also played an important role in lower heat generation and affected the material mixing and stirring efficiency, thus, caused improper material flow. Figs. 2(a) and 2(b) also show non-uniform onion rings. Fig. 2(b) demonstrates smaller surface defects compared to Fig. 2(a), which is attributed to the increase in TRS from 560 rpm to 710 rpm. This leads to higher rotation speed to traverse speed ratio, which was responsible for higher heat generation in accordance to equation 1. Fig. 2 (c) depicts that the 'surface lack of fill' defect has removed at 900 rpm due to higher heat generation but tunnel defect was still there as highlighted in Fig. 2 (d). Onion rings were also become uniform compared to Fig. 2(a) and 2(b), but tunnelling defect may be there due to the TA; 0°. Fig. 3 shows the defect free FSPed sample. Defect removal can be attributed to the given 1.5° TA.

3.2 Microstructural and microhardness Analysis

Following the FSP process at TRS; 900 rpm, TTS; 25mm-min^{-1} and TA: 1.5°, the developed microstructure in Mg-2Zn Mg-alloy isdepicted in Fig. 4. The average grain size (AGS) of refined microstructures calculated utilizing theImageJ softwareand it was recorded as 27.38 µmin SZ, whereas, 63.86 µmin BM. The grain size reducedsignificantly after FSP, dueto dynamic recrystallization, optimum material flow and stirring action. Slight grain refinement has also been observed in HAZ and TMAZ. The pattern of material flow is smooth in SZ as indicated by two circles in Fig. 4. Frictional heat generated at the interface between the tool and the workpiece softens the material, making it more susceptible to deformation. As

per equation (1), this thermal softening was explicitely occured at higher TRS (900 rpm), which facilitated the rearrangement of atoms and dislocations within the material and promoted grain refinement and microstructural homogenization.The average microhardness was calculated by the measurement on top (1), middle (2) and bottom layer (3), which arelabelled on cross-section of processed materialas shown in Fig.5. The locations of microhardness measurement are indicated by‘star’ mark. The average microhardness at different locations of layer 1, 2 and 3 are shown graphically in Fig. 5. The maximum microhardness of 58HV was recorded at the central location in SZ, which is nearly 19% higher thanuntreated material (47 HV). The increase in microhardness can be attributed to plastic deformation, wherein the advancing side (AS) experiences a larger heat input compared to the retreating side (RS) because of the direction of tool rotation. It is clear from Fig. 5 that the microhardness on the AS exhibited better values than the RS. Generally, FSP leads to a higher degree of recrystallization and grain refinement, which can be tailored using properly designed cooling system.

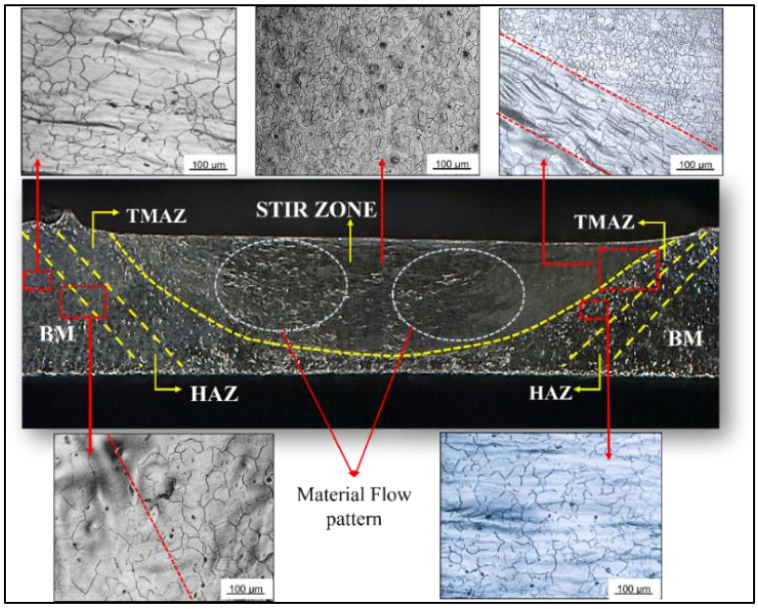

Fig. 4 Microstructural analysis of FSP treated Mg-2Zn Mg-alloy at TRS; 900 rpm, TA; 1.5° (TMAZ-Thermo-mechanically affected zone, HAZ- Heat affected zone, BM- as-cast base material)

3.3 Electrochemical Corrosion Analysis

Corrosion study of 24 hr via potentiodynamic polarization method was accomplished for as-cast BM and FSP treated (TRS; 900 rpm, TTS: 25mm/min., TA; 1.5°) samples. The linear polarization curves of both the samples are manifested in Fig. 6. Table 3 presents a comparison of the corrosion potential (E_{cor}) and corrosion current density (I_{cor}) values.

Table 3. E_{cor} and I_{cor} values for BM and FSPed samples

Sample type	E_{cor} (V)	I_{cor} (A/cm^2)
BM	-1.49	1.98×10^{-4}
FSPed	-1.67	6.92×10^{-4}

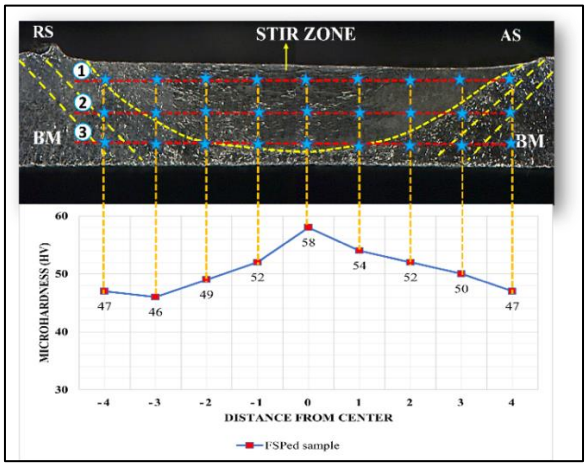

Fig. 5 Average microhardness profile of FSPed sample in processed zone

The E_{cor} of FSP treatedMg-2Zn sample (-1.67 V) has moved towards negative side as compared to BM (-1.49 V), while the I_{cor} value increased to some extent (from $1.98\times10^{-4}$for BM to 6.92×10^{-4}A/cm^2 for FSPed sample).

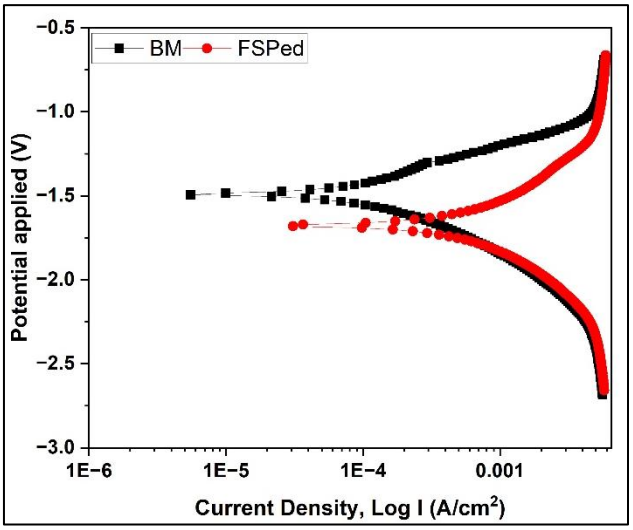

Fig. 6. Electrochemical corrosion behaviour of BM and FSPed sample

The electrochemical corrosion analysis suggests that the FSP treatment deterioratedthe corrosion resistance.This happened because after FSP treatment number of grain boundaries

increased which ultimately worked as corrosion attack sites and expedite thecorrosion phenomenon on FSP treated sample.

Surface morphology of corroded samples was also examined after 24 hr electrochemical corrosion study. Figs. 7 (a) and 7 (b) depict that corrosion products are deposited on the surface of BM and FSPed sample. Figure 7(a) and 7(b) shows that corroded product on the BM surface was on discrete locations, whereas on the FSPed sample surface the corroded product was evenly distributed. This corrosion product will form a passive layer on the FSPed sample and can be helpful in retarding CR of the sample. But this phenomenon was dominated by the increased number of grain boundaries, which resulted as reduced corrosion potential after FSP treatment. The linear polarization curves and surface morphology of the BM and processed samples suggested that a detailed study is needed for the better understanding of corrosion behaviour after FSP.

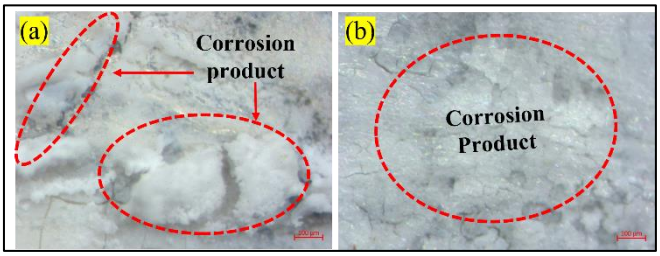

Fig. 7. Corroded product images of (a) BM, (b) FSP treated sample

4 Conclusion and Future scope

The present study conducted on FSP of Mg-2Zn Mg-alloy revealed that:

- The FSP parameters namely TRS; 560 rpm and 710 rpm, along with TA; 0° produced the 'surface lack of fill' defect because of inadequate heat-generation and inappropriate material stirring.
- Defect free microstructure was obtained for FSP treatment with TRS; 900 rpm, TTS; 25mm/min and TA of 1.5°.
- Microstructure analysis portrayed that effective grain refinement from 63.86 µm to 27.38 µm was achieved after FSP treatment and the microhardness was improved from 47 HV to 58 HV.
- Electrochemical corrosion analysis showed that corrosion rate was increased after FSP (E_{cor} was reduced from -1.49V to -1.67 V).

For better understanding of the corrosion behavior of FSP processed Mg-alloys, more detailed corrosion study of prolonged immersion (3-4 weeks) needs to be conducted. The present study was reported at single FSP pass, whereas multiple passes of FSP along with different tool pin geometries can be explored in future to develop surface composites using powder reinforcements.

Acknowledgement. The authors acknowledge Prof. Arshad Noor Siddiquee, Professor,MED, JMI, New Delhi for extending the research support to carry out FSP treatment of Mg-2Zn Mg-alloy.

References

[1] N. Sezer, Z. Evis, S. M. Kayhan, A. Tahmasebifar, and M. Koç:Review of magnesium-based biomaterials and their applications, Journal of Magnesium and Alloys, vol. 6, no. 1. National Engg. Reaserch Center for Magnesium Alloys, pp. 23–43, Mar. 01, 2018. doi: 10.1016/j.jma.2018.02.003.

[2] A. Singh and S. P. Harimkar :Laser surface engineering of magnesium alloys: A review, JOM, vol. 64, no. 6. pp. 716–733, Jun. 2012. doi: 10.1007/s11837-012-0340-2.

[3] G. Sharma, K. Kumar, P. S. Satsangi, and N. Sharma :Surface Modification of Biodegradable Mg-4Zn Alloy Using PMEDM: An Experimental Investigation, Optimization and Corrosion Analysis, IRBM, vol. 43, no. 5, pp. 456–469, Oct. 2022, doi: 10.1016/j.irbm.2021.02.003.

[4] K. Kumar, R. S. Gill, and U. Batra :Challenges and opportunities for biodegradable magnesium alloy implants, Materials Technology, vol. 33, no. 2. Taylor and Francis Ltd., pp. 153–172, Jan. 28, 2018. doi: 10.1080/10667857.2017.1377973.

[5] M. Sankar, J. Vishnu, M. Gupta, and G. Manivasagam :Magnesium-based alloys and nanocomposites for biomedical application, in Applications of Nanocomposite Materials in Orthopedics, Elsevier, 2018, pp. 83–109. doi: 10.1016/B978-0-12-813740-6.00005-3.

[6] G. Eddy Jai Poinern, S. Brundavanam, and D. Fawcett :Biomedical Magnesium Alloys: A Review of Material Properties, Surface Modifications and Potential as a Biodegradable Orthopaedic Implant, Am J Biomed Eng, vol. 2, no. 6, pp. 218–240, Jan. 2013, doi: 10.5923/j.ajbe.20120206.02.

[7] Z. Y. Ma :Friction stir processing technology: A review, Metallurgical and Materials Transactions A: Physical Metallurgy and Materials Science, vol. 39 A, no. 3. pp. 642–658, Mar. 2008. doi: 10.1007/s11661-007-9459-0.

[8] W. Wang et al. : Friction Stir Processing of Magnesium Alloys: A Review, Acta Metallurgica Sinica (English Letters), vol. 33, no. 1. Chinese Society for Metals, pp. 43–57, Jan. 01, 2020. doi: 10.1007/s40195-019-00971-7.

[9] K. Singh, G. Singh, and H. Singh : Review on friction stir welding of magnesium alloys, Journal of Magnesium and Alloys, vol. 6, no. 4. National Engg. Reaserch Center for Magnesium Alloys, pp. 399–416, Dec. 01, 2018. doi: 10.1016/j.jma.2018.06.001.

[10] H. Seifiyan, M. Heydarzadeh Sohi, M. Ansari, D. Ahmadkhaniha, and M. Saremi : Influence of friction stir processing conditions on corrosion behavior of AZ31B magnesium alloy, Journal of Magnesium and Alloys, vol. 7, no. 4, pp. 605–616, Dec. 2019, doi: 10.1016/j.jma.2019.11.004.

[11] N. Saikrishna, G. Pradeep Kumar Reddy, B. Munirathinam, and B. Ratna Sunil : Influence of bimodal grain size distribution on the corrosion behavior of friction stir processed biodegradable AZ31 magnesium alloy, Journal of Magnesium and Alloys, vol. 4, no. 1, pp. 68–76, Mar. 2016, doi: 10.1016/j.jma.2015.12.004.

[12] M. Gao et al. : Influence of microstructure modification on corrosion resistance of friction stir processing biodegradable Mg-Zn-Nd alloy, Materials Technology, vol. 37, no. 1, pp. 57–62, 2022, doi: 10.1080/10667857.2020.1807788.

[13] S. Ahmed, M. V. Malik, and B. Ahmad : Surface moderation and composite fabrication of die-cast magnesium alloys via friction stir processing: a review, Advances in Materials and Processing Technologies. Taylor and Francis Ltd., 2021. doi: 10.1080/2374068X.2021.1970998.